は保たれていた。またオステオポンチンはインテグリンαvβ6を受容体とすることを明らかとした。

D．考察および結論

オステオポンチンの機能の多様性は翻訳後修飾とそれによる受容体の変化に、活性が影響され、また TGFβなどの他の生物活性物質を巻き込んで発揮されているものと考えられた。

F．健康危険情報

特になし。

G．研究発表

1．論文発表

（総説）

1）横崎恭之

気道上皮インテグリンのノックアウトマウスは肺気腫に至る

分子呼吸器病学　8: 10-17 (2004).

（著書）

2）横崎恭之

1-7 細胞接着蛋白質

図説　血栓・止血・血管学、中外医学社、（2004 年印刷中）

2．学会発表など

学会

（国内学会）

1）2003 年 7 月 17 日-18 日　札幌

第 5 回オステオポンチン研究会、

生体防御機能異常ワークショップ

第 6 回肝臓生物研究会

合同年会

横崎恭之、烏帽子田彰

オステオポンチンとインテグリンの相互作用

（基調講演）

2）2003 年 7 月 24 日-25 日　京都

遺伝子診療学会

村上功、横崎恭之、烏帽子田彰

肺癌における分子生物学的異常の治療前診断の試み

3）2003 年 10 月 21 日-24 日　長崎

日本人類遺伝学会

横崎恭之、村上功、佐々木朋宏、田中久美、粟屋智一、東川史子、烏帽子田彰

肺癌・胃癌重複患者で同定されたインテグリンα9サブユニット細胞質ドメインの一塩基置換は機能変化をもたらす

4）2003 年 11 月 8 日　広島

日本老年医学会地方会

横崎恭之、烏帽子田彰

心・血管リモデリング因子オステオポンチンの翻訳後修飾

5）2003 年 12 月 10 日-13 日　神戸

第 26 回日本分子生物学会

横崎恭之、田中久美、山下敬介、烏帽子田彰

オステオポンチンの翻訳後修飾による受容体の変化

6）2004 年 12 月 19 日-20 日　東京

第 3 回分子予防環境医学研究会

横崎恭之、烏帽子田彰
生体反応修飾因子オステオポンチンの機能的多様性とインテグリン

7）2004年3月31日-4月2日
第44回日本呼吸器学会学術講演会
村上功、横崎恭之、重藤えり子
進行非小細胞肺癌患者における遺伝子多型およびp53遺伝子変異の予後的検討

（国際学会）
8）2003年9月16日-18日 Heviz, Hungary
Second Japanese-Hungarian Transglutaminase Conference
Yokosaki Y, Eboshida A
Post-translational modification of osteopontin and transglutaminatioin.

2004年5月22日-27日 Orlando, Florida, U.S.A.
International Meeting of American Thoracic Society
Yokosaki Y, Tanaka K, Yamashita K, Murakami I, Eboshida A, Sheppard D
Interaction of integrin avb6 with osteopontin.

9）2004年5月22日-27日 Orlando, Florida, U.S.A.
International Meeting of American Thoracic Society
Inoue Y, Yamamoto S, Hebisawa A, Yamadori I, Akira M, Arai T, Mochizuki Y, Sato T, Fujita Y, Nagata N, Akagawa S, Saito Y, Maruyama M, Saito T, Eda R, Abe M, Kitada S, Fukushima K, Yokosaki Y, Kobashi Y, Hayashi S, Nagai S, Kitaichi M, Nishimura K, Sakatani M, Travis WD
Prognostic evaluation of radio-pathological findings in fibrotic idiopathic interstitial pneumonitis.

H．知的財産権の出願・登録状況
特になし。

特許
抗オステオポンチン抗体およびその用途（出願）

日本 特願 2002-579907
米国 第10/473,174
ヨーロッパ 第02713293.5号
韓国 第10-2003-7012488
メキシコ 第PA/A/2003/009052号
ブラジル 第4820/03号
チェコ 第PV2003-2697号
オーストラリア 第2002244968号
ニュージーランド 第528483号
インド 第01216/KOLNP/2003号
アルゼンチン 第P02 01 01 262号
台湾 第91106862号

平成１６年度報告書

オステオポンチンの酵素切断による受容体選択性の変化

研究要旨

オステオポンチンは免疫、炎症の調整因子である。その作用は主に受容体インテグリンを介して発揮されるものと考えられるが複数のインテグリンのうち生体内でどれが使用されているか不明である。そこで、オステオポンチンの酵素切断により結合するインテグリンが変化することを確かめた。

A．緒言

酸性糖蛋白オステオポンチンは、細胞外マトリックスにもサイトカインにも分類される多彩な機能を持つ分子である。組織のリモデリングや免疫反応、炎症反応の修飾をおこなうが、その機能は受容体インテグリンあるいは CD44 と結合することによって発揮される。オステオポンチンは多くのインテグリンが好んで結合する RGD 配列を有しており、αvβ1, αvβ3, αvβ5, α5β1, α8β1 がここに結合する。またα4β1 とα9β1 が RGD に隣接した SVVYGLR 配列に結合する。マイクロアレイを使用した近年の報告によれば、オステオポンチン発現は環境刺激により劇的に誘導される。インテグリンαvβ6 も同様に環境刺激で上昇するが、ブレオマイシン刺激におけるオステオポンチン上昇は、αvβ6 欠損マウスでは生じないため、αvβ6 に依存した上昇機構が存在すると考えられる。そこで、今回私たちはオステオポンチンとインテグリンαvβ6 の相互作用に関して検討した。次に、オステオポンチンは生体内で、トロンビン、MMP-3 および MMP-7 により切断されることが示されており、トロンビン配列と MMP-3,7 の切断部位の差はアミノ酸 2 残基と非常に近接している。また MMP-3,7 の切断部位は上記の SVVYGLR 配列の中にある。従って、これらの切断により、結合できる受容体の種類が変化すると仮説をたて、切断型のリコンビナント蛋白を作製し結合性を検討した。

B．方法

全長オステオポンチン cDNA に deletion mutation を施し、酵素分解産物をコードした cDNA を作製し、発現ベクターに組み込み大腸菌に GST 融合蛋白として発現させ精製した。オステオポンチンとインテグリンの結合は、インテグリンα9, β3, β6 cDNA を遺伝子導入した SW480 細胞を用い、SW480 の発現するオステオポンチン受容体、αvβ5, α5β1 の阻害抗体存在下で接着アッセイを行った。また、αvβ6 とオステオポンチンの結合はオステオポンチンを結合させたカラムを作製し、可溶性αvβ6 の結合性を確かめた。

C．結果および考察

可溶型αvβ6 はオステオポンチンカラムから EDTA により溶出され、このインテグリンがオステオポンチンの受容体であることを新しく同定した。また、RGD 配列近傍の配列を変化させる事により、αvβ5, αvβ6 の結合性は大きく低下したが、αvβ3, α5β1 は変化を認めなかった。トロンビン切断型は全長型に比べて、αvβ3, αvβ5, αvβ6 との結合性は著変なかったが、α5β1, αvβ5 の結合性は大きく上昇していた。一方、MMP 切断型では、α5β1, αvβ5 の結合性は低下していた。以上より、全長オステオポンチンに対しては、αv-インテグリンが (RGD 部位のコンフォメーションによってはαvβ3 優位に) 働き、トロンビン存在下ではα5β1, α9β1 が働き、MMP 存在下では、またαv-インテグリン優位となるものと考えられた。オステオポンチンのインテグリンとの結合性は酵素の翻訳後修飾により変化し、その機能に影響を与える物と考えられた。

D．文献

1. Yokosaki Y, et al: *J. Biol. Chem.* 274: 36328-36334, 1999.
2. Yokosaki Y, et al: *Trend. Cardiovasc. Med* 10: 155-159, 2000.
3. Yokosaki Y, et al: *Matrix biology* (in press)
4. 横崎恭之他、日本臨床（印刷中）

Ｅ．健康危険情報
なし

Ｆ．研究発表
Ｆ－１．論文発表
1) Yokosaki Y, Tanaka K, Higashikawa F, Yamashita K, Eboshida A
Distinct structural requirements for binding of the integrins alphavbeta6, alphavbeta3, alphavbeta5, alpha5beta1 and alpha9beta1 to osteopontin'
Matrix Biology（印刷中、2005）
2) 横崎恭之、東川史子
日本臨床特集号：臨床分子内科学３
VII.特論　オステオポンチン
オステオポンチン受容体とシグナル伝達。
日本臨床（印刷中、2005）

Ｇ．知的財産権の出願・登録状況
なし。

ＩＩＩ．研究成果の刊行に関する一覧表

ア）　主任研究者：山下敬介

1）Yamashita K (2002) Fine structural aspects of the urothelium in the mouse ureter with special reference to cell kinetics. Hiroshima Journal of Medical Sciences 51 (2): 41-48. （原著論文）

2）Morita M, Kobayashi A, Yamashita T, Simanuki T, Nakajima O, Takahashi S, Ikegami S, Inokuchi K, Yamashita K, Yamamoto M, Fujii-Kuriyama Y (2003) Functional analysis of basic transcription element binding protein by gene targeting technology. Molecular and Cellular Biology 23 (7): 2489-2500. （原著論文）

イ）　分担研究者：菅野雅元

3）Sakai R, Kajiume T, Inoue H, Kanno R, Miyazaki M, Ninomiya Y, Kanno M (2003) TCDD treatment eliminates the long-term reconstitution activity of hematopoietic stem cells. Toxicological Sciences 72: 84-91. （原著論文）

ウ）主任研究者：山下敬介

4) Sugihara K, Kitamura S, Yamada T, Okayama T, Ohta S, Yamashita K, Yasuda M, Fujii-Kuriyama Y, Saeki K, Matsui S, Matsuda T (2004) Aryl hydrocarbon receptor-mediated induction of microsomal drug-metabolizing enzyme activity by indirubin and indigo. BBRC 318: 571-578. （原著論文）

5）Fukui Y, Ema M, Fujiwara M, Higuchi H, Inouye M, Iwase T, Kihara T, Nishimura T, Oi A, Ooshima Y, Otani H, Shinomiya M, Sugioka K, Yamano T, Yamashita KH, Tanimura T (2004) Comments from the behavioral teratology committee of the Japanese Teratology Society on OECD guideline for the testing of chemicals, proposal for a new guideline 426, developmental neurotoxicity study, draft docu;ment (September 2003). Cong. Anom. 44: 172-177. （原著論文）

エ）分担研究者：横崎恭之

6）横崎恭之 (2004) 気道上皮インテグリンのノックアウトマウスは肺気腫に至る。分子呼吸器病 8(1): 10-17. （原著論文）

7) Yokosaki Y, Tanaka K, Higashikawa F, Yamashita K, Eboshida A (2005, in press) Distinct structural requirements for binding of the integrins $\alpha v\beta 6$, $\alpha v\beta 3$, $\alpha v\beta 5$, $\alpha 5\beta 1$ and $\alpha 9\beta 1$ to osteopontin. Biomatrix Biology. （原著論文）

8）横崎恭之、東川史子 (2005 印刷中) オステオポンチン受容体とシグナル伝達。
Osteopontin receptors and signal transduction. 日本臨床 臨床分子内科学３
VII.特論 －オステオポンチン－ （原著論文）

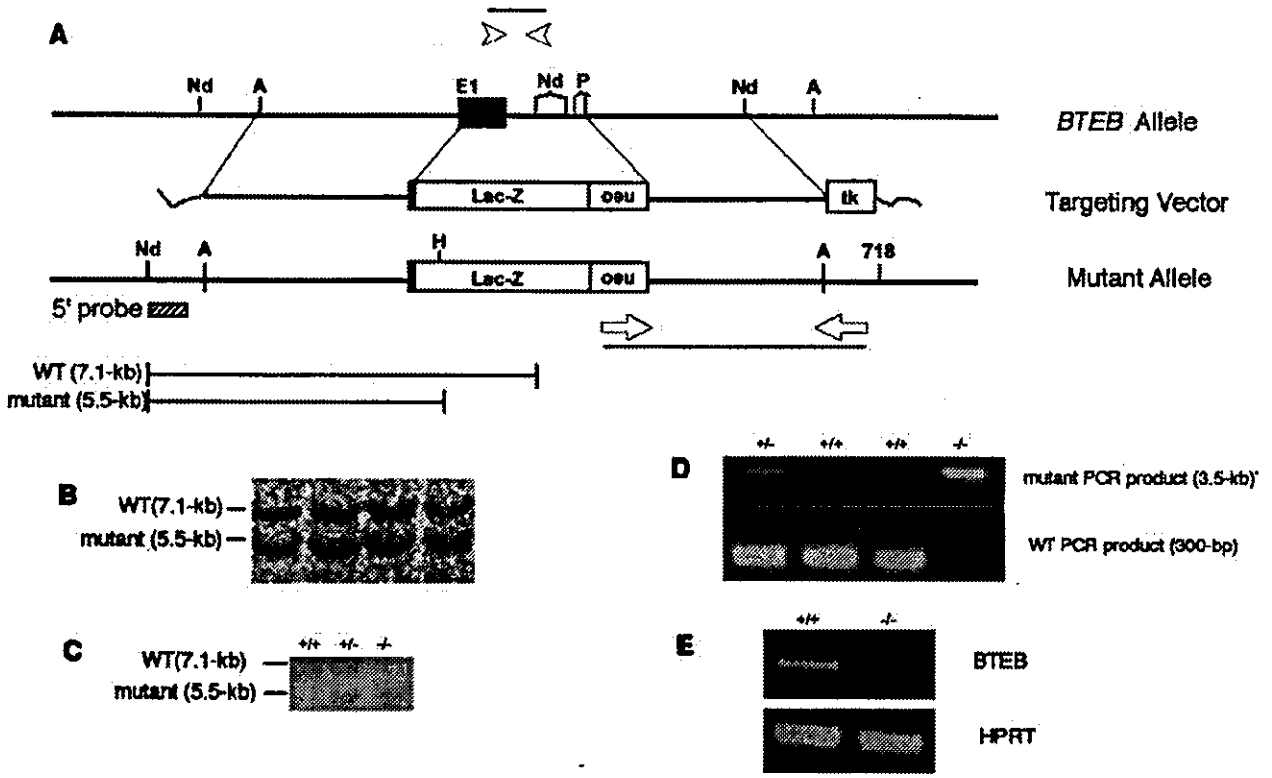

FIG. 1. Mutation of mouse *BTEB* gene. (A) Outline of targeting vector and restriction maps around the first exon. Arrowheads indicate the sites of primers used to distinguish the wild-type BTEB gene from that of the mutant. neo indicates the neomycin-resistant gene, and tk is the thymidine kinase gene under the control of the herpes simplex virus promoter. The sizes of the DNA fragments digested with *Nde*I are shown below. (B and C) DNA blot analysis of DNA from recombinant cells and mouse tails, respectively. Genomic DNAs were prepared from ES cells and mouse tail, digested with *Nde*I and *Hin*dIII, and electrophoresed in 1% agarose, followed by hybridization with the 5′ probe indicated in panel A. (D) Genotyping of the BTEB locus from offspring. PCR analyses were carried out with genomic DNAs from offspring generated by cross-mating heterozygous $BTEB^{+/-}$ mice. The primer pairs were used as described in panel A, and the PCR products were analyzed by agarose gel electrophoresis. (E) RT-PCR analyses of BTEB mRNA expression. RNAs were prepared from the brains of wild-type and mutant mice. RT-PCR of the prepared RNAs was performed with a pair of primers as described in Materials and Methods, and the RT-PCR products were separated by agarose gel electrophoresis. hypoxanthine phosphoribosyltransferase (HPRT) mRNA expression was used as control.

To investigate the functional role of BTEB per se and at least a part of T_3 effects on mouse brain development, we generated BTEB gene knockout mice. The *lacZ* gene was inserted into the reading frame of the first exon in BTEB gene by homologous recombination, such that β-galactosidase (β-Gal) expression mimics the expression of BTEB, thereby facilitating the survey of pathological abnormalities due to a lack of BTEB expression.

Homozygous BTEB knockout ($BTEB^{-/-}$) mice were bred by apparently normal Mendelian genetics from a cross between heterozygous $BTEB^{+/-}$ mutant mice and grew normally and were fertile. Expression of BTEB dramatically increased in the brain, especially in the hippocampus and cerebellum, at around postnatal day 7 (P7), the time when synapses begin to mature in the CNS. Examination of general locomotor activities, motor coordination, and memory tasks revealed that BTEB mutant mice exhibit deficits in motor coordination and in learning and memory tasks, which are principally associated with cerebellar and hippocampal functions, respectively.

MATERIALS AND METHODS

Construction of targeting vector. A genomic DNA sequence containing the 5′-flanking region and the first intron of the BTEB gene was isolated from a mouse 129/SV genomic library, with rat BTEB cDNA *Sac*II-*Nsp*V fragment used as a probe. An *Ase*I/*Not*I fragment of 5 kb containing the BTEB promoter and 12 bp of the coding sequence of the first exon was fused in frame with the *lacZ* cassette (*Hin*dIII/*Sma*I fragment of pENL) containing the simian virus 40 T antigen intron and the polyadenylation signal. The 3′ end of the *lacZ* cassette was fused with the *neo* gene cassette (*Xho*I/*Bam*HI fragment of pMC1-neo) in a reverse orientation to the *lacZ* gene for the positive selection, followed by 3.1 kb of a *Pvu*II/*Ase*I fragment of the mouse BTEB gene. This construct was ligated to the thymidine kinase cassette (HSV-TK) at the 3′ end and inserted between the *Eco*RV and *Asp*718 sites of pBluescript for amplification in *Escherichia coli*. The amplified plasmid was linearized by *Kpn*I digestion and used for electroporation.

Targeted disruption of the BTEB gene in ES cells. E14 embryonic stem (ES) cells were cultured, transformed with the targeting vector, and screened by standard methods (9). The linearized targeting vector DNA (80 μg) was electroporated into ES cells (10^7 cells/ml), and the cells were subjected to double selection by using G418 (300 μg/ml) and ganciclovir (2 μM). After 10 days, isolated clones were expanded and genomic DNAs were prepared for determination of homologous recombination.

Blastocysts were harvested from 3.5-day postcoital (dpc) C57BL/6j females and the homologous recombinant ES cells were injected into the blastocoel

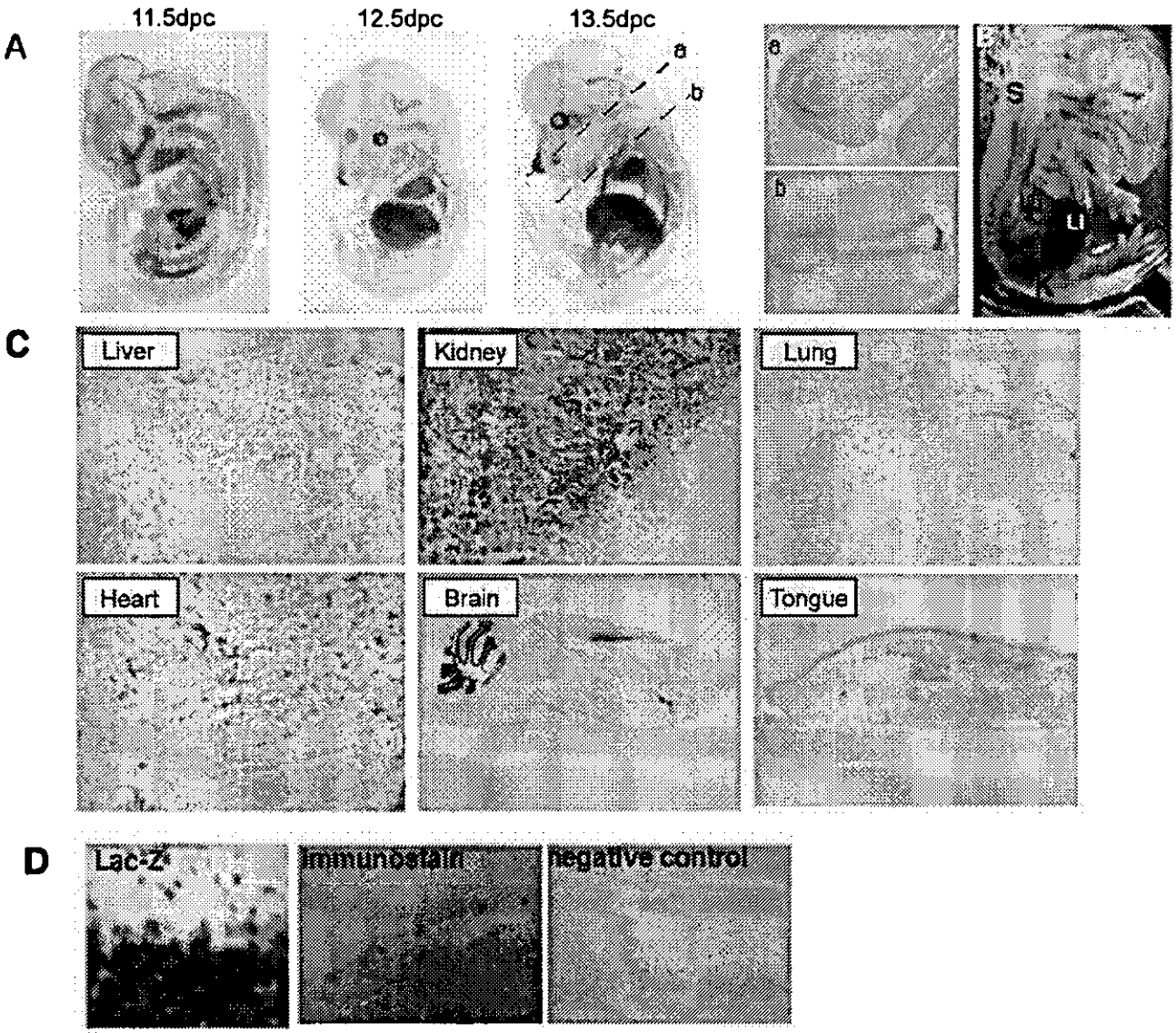

FIG. 2. Expression patterns of BTEB in mouse embryo and adult tissues. (A) Until 11.5 dpc, BTEB was not detected in any organ in mouse embryo. BTEB expression started at 12.5 dpc, and expression was restricted to skeletal tissue. The photos in subpanels a and b are sections indicated by broken lines of BTEB$^{+/-}$ 13.5-dpc embryo with β-Gal staining. Sections a and b show BTEB expression in the cartilage primordium of nasal capsule and the cartilage primordium of rib, respectively. (B) At 15.5 dpc, BTEB expression extended to the spinal cord, kidney, and lung. (C) BTEB expression in adult mouse tissues was detected rather ubiquitously in various tissues, such as liver, kidney, heart, brain, and tongue tissues. Lung tissue was the only tissue for which we could not detect BTEB expression in adult mice and only a weak expression at the embryonic stage. (D) β-Gal expression of the cerebellum in BTEB$^{+/-}$ mice showed almost the same expression pattern as observed with immunostaining with anti-BTEB antibody. A P14 BTEB$^{+/-}$ mouse cerebellum sagittal section was stained with β-Gal, and a BTEB$^{+/-}$ cerebellum sagittal section was analyzed by using immunohistochemistry with anti-BTEB antibody. Both β-Gal staining and immunostaining showed identical positive signals in Purkinje cells and the granular cell layer. The negative control for immunohistochemistry was performed with nonimmune serum (right photo). Abbreviations: S, spinal cord; Lu, lung; K, kidney; Li, liver.

cavities of the 3.5-dpc blastocysts. Injected blastocysts were surgically transferred into uteri of 2.5-dpc pseudopregnant Jcl:ICR mothers (9). Male chimeric pups with an extensive ES cell contribution to their coat color were bred with C57BL/6j females, and germ line transmission of the dominant agouti color marker was assessed in the resulting offspring. Germ line transmission of the defective BTEB allele was screened by the PCR method and subsequently confirmed by DNA blot analysis by using DNA prepared from tails. The primer pair and DNA probe used for the PCR and the DNA blot analysis, respectively, were as follows: the *neo* sequence at the 5′ end, 5′-CAG TCA TAG CCG AAT AGC CTC TCC ACC CAA-3′, and the endogenous BTEB-flanking sequence at the 3′ end, 5′-CAG TCA TAG CCG AAT AGC CTC TCC ACC CAA-3′ for PCR and the *NdeI-AseI* fragment (1 kb) for DNA blot analysis. PCR analysis consisted of 30 cycles of 98°C for 20 s, 60°C for 45 s, and 68°C for 3 min with LA *Taq* (TaKaRa, Tokyo, Japan). For DNA blot analysis, tail DNAs were digested with *Nde*I and *Hin*dIII and subjected to 1% gel electrophoresis for blot hybridization.

β-Gal staining and TUNEL (terminal deoxynucleotidyltransferase-mediated dUTP-biotin nick end labeling). β-Gal staining was carried out as described previously (9), with embryos or adult tissues fixed in phosphate-buffered saline (PBS) containing 2% paraformaldehyde, 0.2% glutaraldehyde, and 0.05% Non-

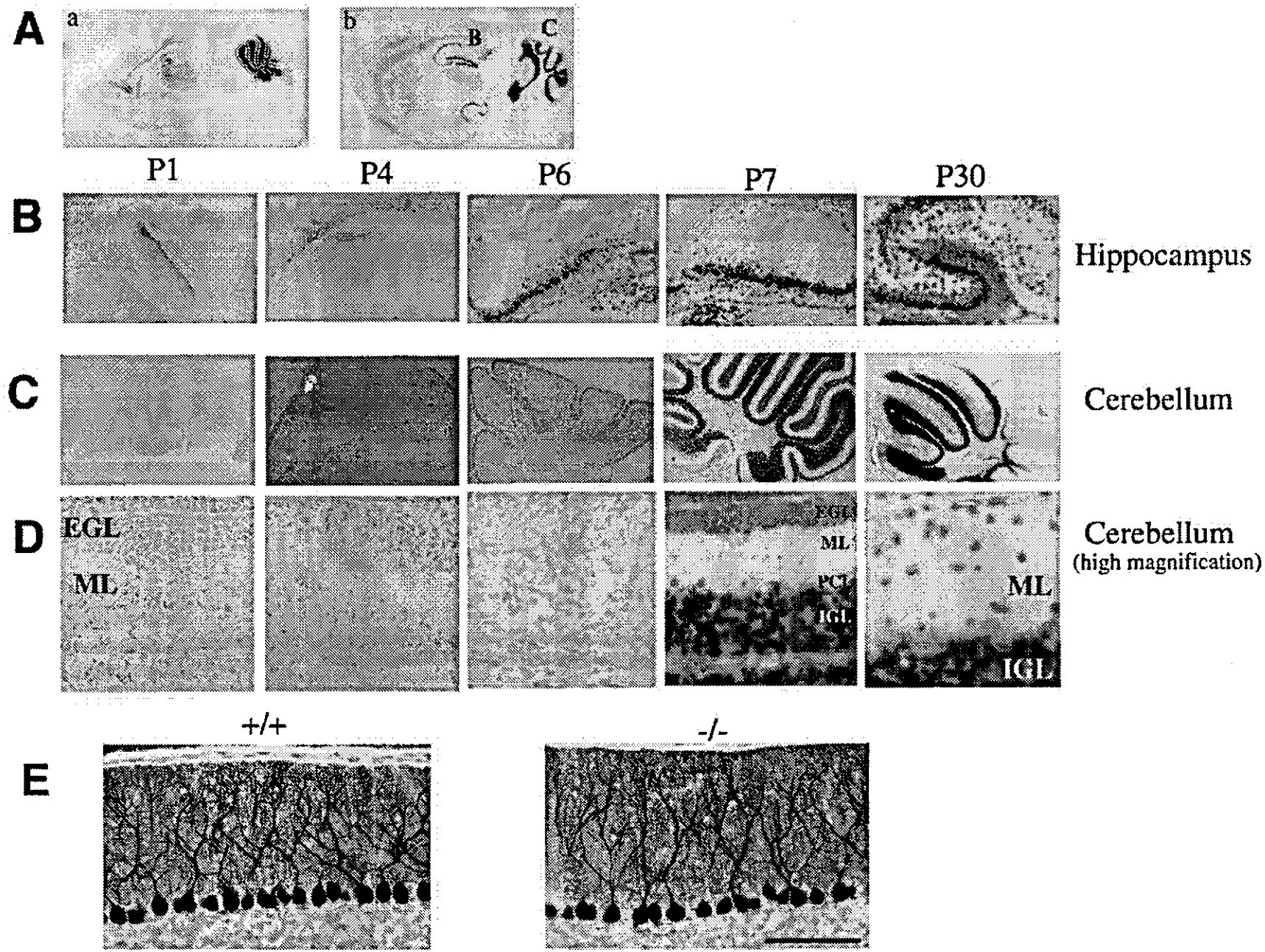
A
a
b
B
C
P1
P4
P6
P7
P30
B
Hippocampus
C
Cerebellum
D
EGL
ML
EGL
ML
PCL
IGL
ML
IGL
Cerebellum
(high magnification)
E
+/+
-/-

FIG. 3. Spatiotemporal expression pattern of BTEB in the developmental process of mouse brain. β-Gal staining was performed with the brain of BTEB$^{+/-}$ heterozygous mice from stage P1 to P30. (A) Sagittal sections of brain from BTEB$^{+/-}$ heterozygous mutant mice at P7 (a) and P30 (b). The "B" and "C" labels in subpanel b indicate the areas of BTEB expression investigated in 3B (hippocampus) and 3C (cerebellum), respectively. (B) Temporal expression of BTEB in hippocampus at various postnatal stages. Heterozygous BTEB$^{+/-}$ mice were killed at P1, P4, P6, P7, and P30. Brains were removed and fixed for β-Gal staining. The brain specimens were cut at 10 μm. (C) Temporal expression pattern of BTEB in mouse cerebellum at various postnatal stages. The mouse brains were treated as described in panel B. BTEB expression was not detected during early postnatal stages but was detected distinctly at P7. (D) Magnified views of a part of cerebellar specimens in panel C. At P7, BTEB expression started in the external granular layer (EGL), the Purkinje cell layer (PCL), and internal granular layer (IGL). By P30, migration of external-granular-layer cells to the internal granular layer was complete. BTEB expression in the internal granular layer was preserved at P30, whereas its expression faded in the Purkinje cell layer. ML, molecular layer. (E) Cerebellum sections of wild-type mice and homozygous BTEB mutant mice were stained with anti-IP$_3$R1 antibody to analyze the structure of Purkinje cells. Stained areas show dendritic shafts and spines of Purkinje cells.

idet P-40. For detection of β-Gal, specimens were soaked in PBS containing 20% sucrose, embedded in Tissue-Tek OCT compound (Sakura, Tokyo, Japan), and frozen in liquid nitrogen. Specimen sections of 30 μm were cut in a cryostat.

The TUNEL method was performed to detect apoptosis in brains according to the manufacturer's instruction (TaKaRa). Brains (P7) were fixed in neutralized formalin. Paraffin sections (3 μm) were subjected to the TUNEL experiment by using the in situ apoptosis detection kit (TAKARA).

Immunohistochemistry. Development of Purkinje cells was studied by immunostaining with an anti-IP$_3$R1 (1,4,5-inositol trisphosphate receptor 1) antibody. Dissected brains were fixed in Boun's solution for 2 h. Paraffin sections (8 μm thick) in the parasagittal plane were processed sequentially as described previously (27).

RNA analysis. mRNAs were analyzed by the reverse transcription-PCR (RT-PCR) method as described previously (28). Total RNA was prepared from mouse brains and aliquots (1 μg/ml) were reverse transcribed with random primers at 37°C for 60 min. The reverse transcripts were quantified by the PCR method. An aliquot (1 μl) of synthesized cDNA was amplified in a total volume of 20 μl containing 150 mM deoxynucleoside triphosphates, 0.2 U of *Taq* polymerase, and 0.12 μg of each pair of primers described below and [α-^{32}P]dCTP (4 μCi/20 μl). For BTEB, the 5′ and 3′ primers were 5′-ATG TCC GCG GCC GCC GCC GCC TAC AT-3′ and 5′-TCT GCA CTG TGG GAG GCC AG-3′, respectively. For β-actin control, the 5′ and 3′ primers were 5′-ATG GAT GAC GAT ATC GCT-3′ and 5′-ATG AGG TAG TCT GTC AGG 4T-3′, respectively. PCR was performed as 30 cycles of 30 s at 94°C, 30 s at 60°C, and 1 min at 72°C. The PCR products were analyzed on a 1% agarose gel with β-actin as a control.

Treatment of mice. In all experiments, littermates from cross-mating between BTEB$^{+/-}$ mice were used, and their genotypes were determined by PCR analysis of tail DNA samples. All of the mice used for the experiments were 10- to 15-week-old males. The mice were kept on a 12-h light-dark cycle at a constant temperature (23 ± 1°C). The tests were always conducted between 13:00 and 18:00. A week prior to the behavioral tests, one mouse was housed per cage and handled three times daily.

General activity. Locomotion and rearing behavior were measured by the method described previously (12) in an open-field box (32 by 32 by 20 cm) placed in a sound-attenuated room that was different from the room used for fear conditioning. Two pairs of a 7-by-7 array infrared photosensors were set against the outer wall and equally spaced in the lower and upper rows at intervals of 2 and 4.5 cm, respectively, above the floor. The frequency at which a photobeam was interrupted represented the movement of the animal and was recorded by computer. Each mouse was kept in the box for 30 min.

Light-dark choice test. The apparatus consisted of two compartments and was placed in a dark and sound-attenuated room. One compartment was a bright (250 lx) chamber of 16 by 32 by 20 cm illuminated by a white bulb (60 W), and the other was a dark (1 lx) chamber of the same dimensions. The two compartments were separated by a wall and connected by seven small openings (3 by 9 cm) through which the photobeam sensors passed. A mouse was placed in the center of the light chamber and its behavior was monitored by video camera. The mouse was considered to have entered the new area when all four feet were placed in that area. The following behavioral measures were scored: the time spent in the light and dark compartments, the number of transitions made between the two compartments, and the latency of the initial movement from the light to the dark room.

Rotorod test. The rotorod test was carried out as described previously (6). Mice were placed on a rod and the rod began to rotate at a constant velocity of 15 rpm. The test was continued for 3 min. The time that the mouse stayed on the rotating rod was measured. The test was done once a day for each mouse and repeated for 5 days.

Contextual fear conditioning. The experiment of contextual fear conditioning was performed as described previously (13). The conditioning chamber was an observation box (20 by 20 by 20 cm) constructed from clear and gray vinylchloride plates. The floor of the chamber consisted of 26 stainless steel rods through which foot shocks were delivered by means of a shock scrambler (SGS 002; Muromachi, Tokyo, Japan). The chamber was placed in a light and sound-attenuated room. A video camera placed in front of the chamber allowed the behavior of each mouse to be observed and recorded in an adjacent room. The shock scrambler and controller for conditioning was operated by remote in the same room. On the training day, each mouse was placed in the chamber for 2.5 min before it received three foot shocks (0.5 mA for 1 s with 2-min intervals). The mice were removed from the chamber 1 min after the last foot shock and returned to their original cages. At 24 h after training, the mice were returned to the chamber, and their behavior over a period of 6 min was observed in the absence of foot shocks. The extent of conditioned fear was measured by scoring the freezing behavior of the mice. Freezing was defined as the absence of visible

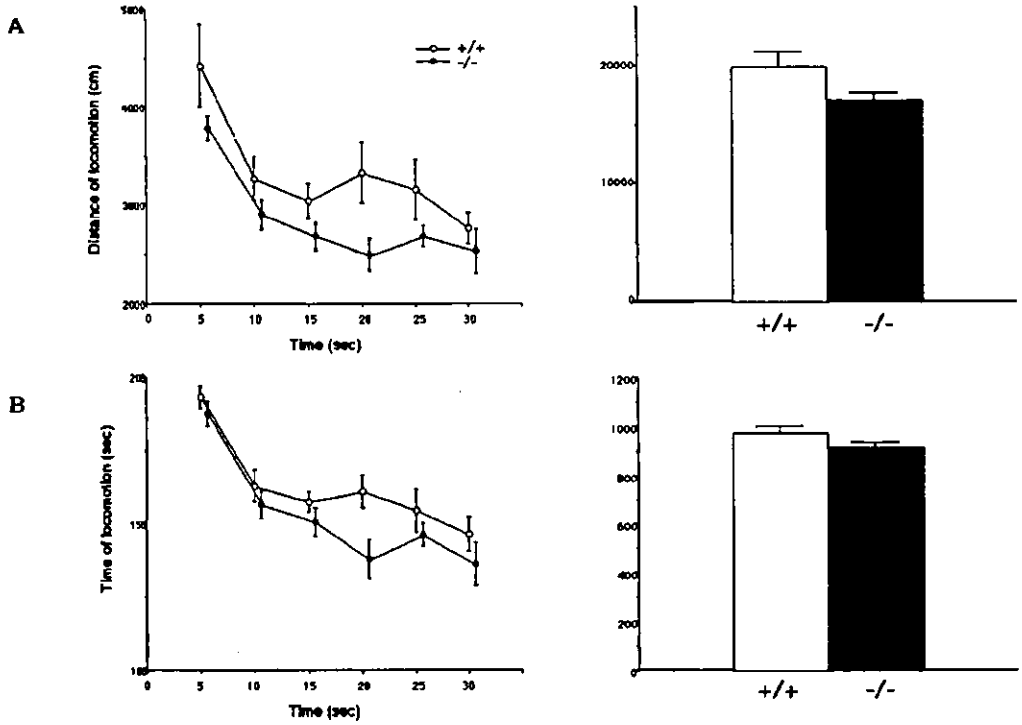

FIG. 4. Locomotion behaviors of BTEB$^{-/-}$ homozygous mutant and wild-type mice. Distance traveled during locomotion (A), time spent for horizontal movement (movement of more than 1 cm/s was counted) (B), frequency of rearing behavior (counts) (C), speed of movement (D), and the time spent in the light and dark compartments (E) for the preceding 5 min were measured and plotted for the total 30 min in the open-field test. Two pairs of array infrared photosensors were attached to the outer wall equally spaced in lower and upper rows, respectively, 2 and 4.5 cm above the floor. The lower row of photocells was used to measure locomotor activities, and the upper row was used to detect rearing behavior. A computer recorded the number of horizontal photobeam interruptions caused by animal movement. Each mouse was placed in the apparatus and left for 30 min, which was approximately the same time as when it received training trials in the afternoon. The points in the left panels show the average values of the locomotor activities for each 5 min in 30 min, and the bar graphs (right) show the average values of the total activities for 30 min with minimum deviation. In each experiment, wild-type mice (n = 9) and homozygous mutant mice (n = 11) were used.

movement, except for respiration. During the test period, two observers who were blind to the experimental conditions scored the tendency of the mice to freeze by watching the TV monitor. Observations were carried out by using a time-sampling procedure. For every 5 s during the test, the movement of each mouse was judged as either frozen or active. An unbiased estimate of the actual time spent in the frozen position was calculated per minute. After completion of the first fear conditioning test, the mice were returned to their original cages for 24 h and then subjected to a second contextual fear test carried out in the same way as the first.

Electric shock sensitivity test. Since the sensitivity to foot shocks may affect freezing responses, we measured the minimal level of current required for mice to elicit vocalization and jumping by the method described previously (12) after general activity and light-dark choice tests.

Each mouse was placed in the chamber used for the contextual fear conditioning and delivered 1-s shocks of increasing intensity. The interval between shocks was 10 s. The sequence of current used was as follows: 0.05, 0.08, 0.1, 0.2, 0.3, 0.4, 0.5, 0.6, and then 0.8 mA. The minimal level of current required to elicit vocalization and jumping was determined. These experiments were performed in a blind manner.

Other activity tests. The horizontal wire-hanging, rod-walking, and gait tests were performed as described previously (13).

Data analysis. Data were analyzed by one- or two-way analysis of variance, and comparison of the paired groups was carried out by the Fisher latest significant difference test. All values in the text and figure legends are expressed as mean values ± the standard errors of the mean, where n is the number of mice tested.

RESULTS

Targeted disruption of the BTEB gene. Part of the 129/SV mouse BTEB genomic fragment of the targeting vector was replaced by *lacZ* positioned in frame with the BTEB gene. By this means, β-Gal expression mimics the mode of BTEB expression in the homologous recombinant mice and, therefore, facilitates assessment of pathological defects owing to a disrupted BTEB gene (Fig. 1A). The linearized plasmid was introduced into E14 ES cells by electroporation, and the cells were subjected to double selection by using G418 and ganciclovir. PCR analysis and subsequent DNA blot analysis of the DNAs extracted from the resistant clones revealed that, of 268 clones screened, 10 represented legitimate homologous recombination (Fig. 1B). Mutant ES cells were proliferated and microinjected into C57BL/6j blastocysts to give rise to chimeric animals, as judged from coat color. Male chimeras were mated with C57BL/6j females to give heterozygotes possessing the BTEB gene, which were then interbred to yield homozygous BTEB$^{-/-}$ mutant mice. DNA blot analysis with genomic tail DNAs from 103 offspring born from heterozygous matings revealed that the ratio of wild-type BTEB$^{+/+}$ to heterozygous BTEB$^{+/-}$ to homozygous BTEB$^{-/-}$ mice was 27:54:22, which represents the 1:2:1 ratio expected from the normal Mendelian rule (Fig. 1C and D). Homozygous mutant BTEB$^{-/-}$ mice appeared to grow normally and were fertile without any evident pathological defects, indicating that the BTEB gene is not essential for survival or fertility. BTEB mRNA levels were not

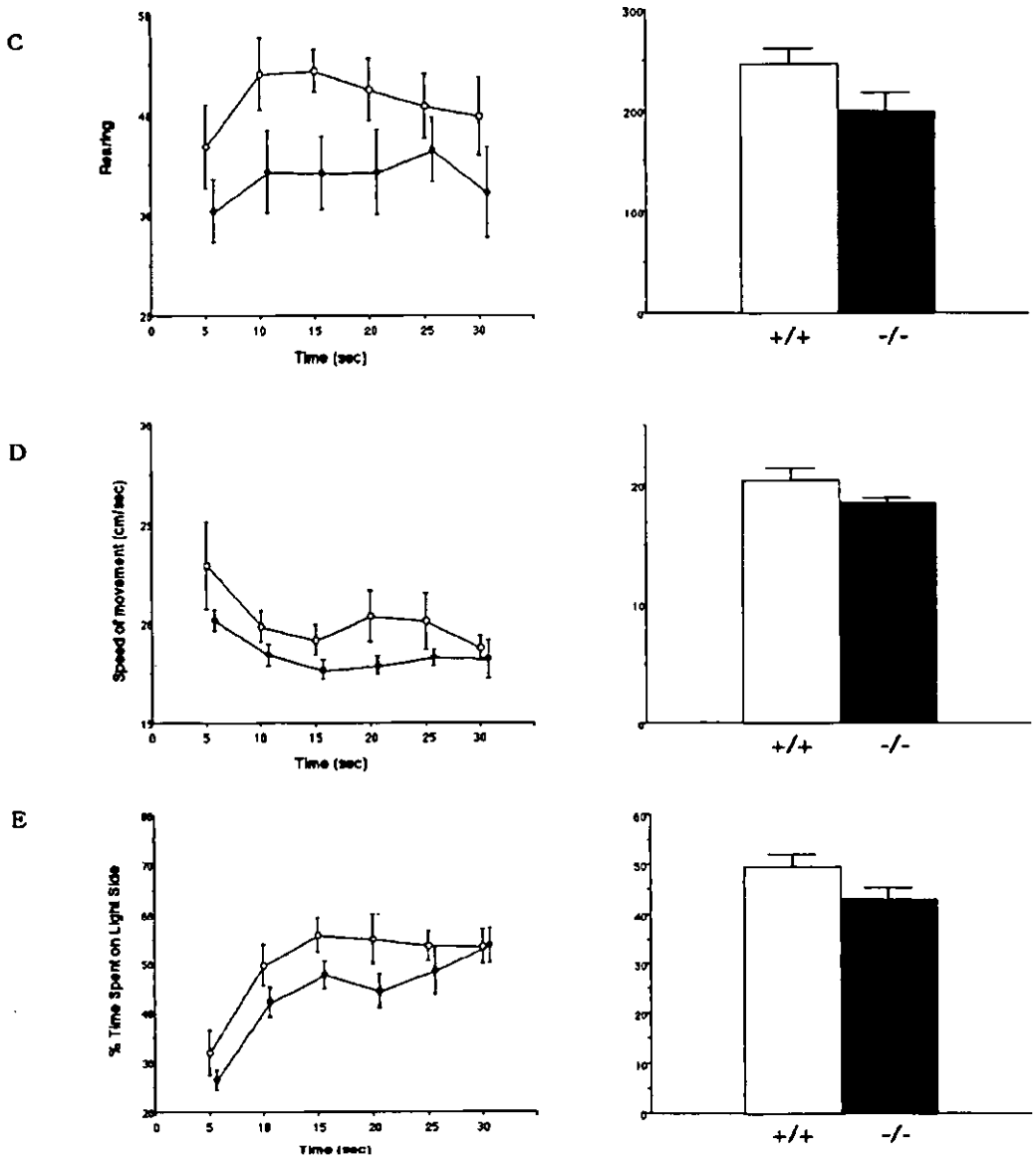

FIG. 4—*Continued.*

detected by RT-PCR analysis with RNA isolated from the brains of adult mutant BTEB$^{-/-}$ mice, indicating perfect disruption of the BTEB gene (Fig. 1E).

Expression of BTEB as revealed by in situ hybridization and β-Gal staining. To investigate the expression pattern of BTEB, we compared β-Gal staining with immunoblot analysis of BTEB with an anti-BTEB antibody at various embryonic stages. The pattern of immunostaining of BTEB generally concurred with that of β-Gal staining (Fig. 2D). Hence, we investigated the expression of BTEB by β-Gal staining. Expression of β-Gal in BTEB$^{+/-}$ mice was essentially the same as that in BTEB$^{-/-}$ mice, indicating that homozygous deletion of the BTEB gene does not result in gross alterations in the formation and development of various organs and tissues. The β-Gal staining revealed that BTEB expression commenced in skeletal structures at E12.5 and spread ubiquitously throughout various tissues except lung (Fig. 2Aa, Ab, and C). In particular, BTEB showed a very characteristic and potent regional expression in the brain (Fig. 3A). BTEB expression was detected in the hippocampus from P1 and was distinctive in the pyramidal cell layer at P6, and significant expression occurred in the cortical layer of the cerebellum at P7, whereas its expression was rather limited in Purkinje cells (Fig. 3B, C, and D). Taken together with the report that forced expression of BTEB by DNA transfection experiments induced the outgrowth of dendrites in Neuro-2A cells, the dynamic expression of BTEB in the developing mouse brain led us to consider that BTEB might be important in the formation of the cerebellum. We compared

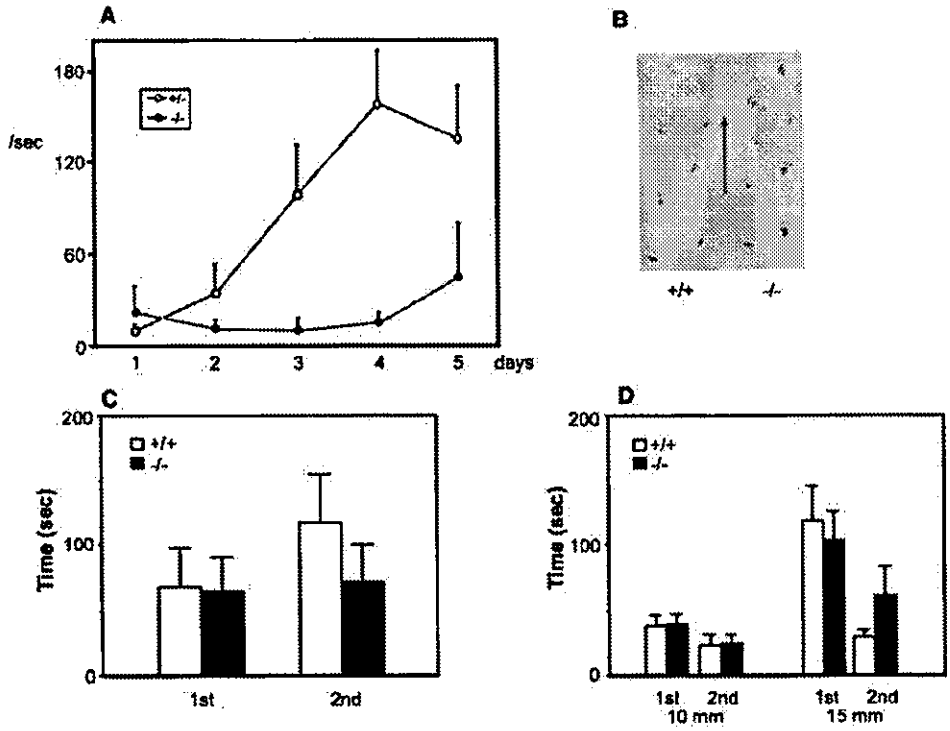

FIG. 5. Rotorod performance in BTEB$^{-/-}$ mutant and wild-type mice. (A) Rotorod test. Fall latencies of the mutant BTEB$^{-/-}$ and wild-type mice on a rod rotating at 15 rpm was measured for 1 s once a day for a consecutive 5 days. Wild-type (n = 9) and mutant mice (n = 11) were used. A maximum of 180 s was tested for each animal per trial. (B) Gait measurement. Representative foot spots of heterozygous and homozygous mutant mice are presented. (C) Horizontal wire-hanging test. Mice were hung on the elevated horizontal wire by the forepaws, and the time in seconds of their hanging on the wire was measured until they fell off the wire. (D) Rod-walking test. Mice were placed on the midpoint of the wooden rod (10 or 15 mm diameter, 60 cm in length), and the time in seconds required for the mice to cross the rod wire was measured. At least nine animals were tested for each genotype.

the morphology of the BTEB$^{-/-}$ cerebellum with that of the wild type by using anti-IP$_3$R1 antibody. Although no marked difference was found between the BTEB-null and the wild-type mice (Fig. 3E), there appeared to be a slightly poorer development of Purkinje cell dendrites in the BTEB-null mice. We performed the TUNEL assay of the cerebellum specimens of the wild-type and the homozygous mutant mice at P7 to see whether apoptosis may occur in this tissue of the mutant mice. However, no noticeable apoptosis signal was found in this tissue of either mutant or wild-type mice at P7 (data not shown). Dendrite development of Purkinje cells in the BTEB-null mice needs to be investigated in a more quantitative manner.

Behavioral assessment of BTEB$^{-/-}$ mutants. From the expression mode of BTEB during mouse brain development and from the transcriptional function of BTEB as a target of T_3, we postulated the involvement of BTEB in learning and memory tasks associated with hippocampal function and in motor coordination related to cerebellar function. We performed systematic analysis of the gross neurogenic and motor functions in BTEB$^{-/-}$ mice.

(i) General activity. We measured, as the basis of the behavioral tests, general activities such as locomotion (distance and time), rearing, speed of movement, and choice between light and dark (Fig. 4). The mean activity counts of locomotion and rearing behaviors for 30 min are shown in Fig. 4. These activities of locomotion and rearing behavior appeared to be slightly lower in homozygous mutant BTEB$^{-/-}$ mice than in wild-type mice (19,988.4 ± 77.8 cm and 248.8 ± 21.5 for the wild type and 17,086.5 ± 74.5 cm and 202.3 ± 22.4 for the mutant mice, respectively). However, analysis of variance indicated insignificant differences in the locomotor activity [$F(1,108) = 14.66$, $P < 0.001$] and rearing behavior [$F(1,108) = 14.89$, $P < 0.001$] between wild-type and BTEB$^{-/-}$ mice, so we did not expect this mild impairment in general activities to greatly influence other behavioral tests (Fig. 4)

Any difference in the internal emotion between wild-type and BTEB$^{-/-}$ mice might affect their performance in the contextual fear conditioning test. Therefore, we carried out a light-dark choice test (Fig. 4E), considered to be a measure of anxiety or fear-related emotion in rodents. The mean percent time spent in the light side was as follows: 50% ± 2% for wild-type mice and 44% ± 2% for BTEB$^{-/-}$ mice. These data were not considered to be significantly different between wild-type and BTEB$^{-/-}$ mice, suggesting that BTEB$^{-/-}$ mice do not have a severe emotional disorder related to anxiety and fear.

(ii) Rotorod test. Since BTEB was clearly demonstrated to be expressed in Purkinje cell layers of the cerebellum (Fig. 3), we carried out the rotorod task, which is associated with cer-

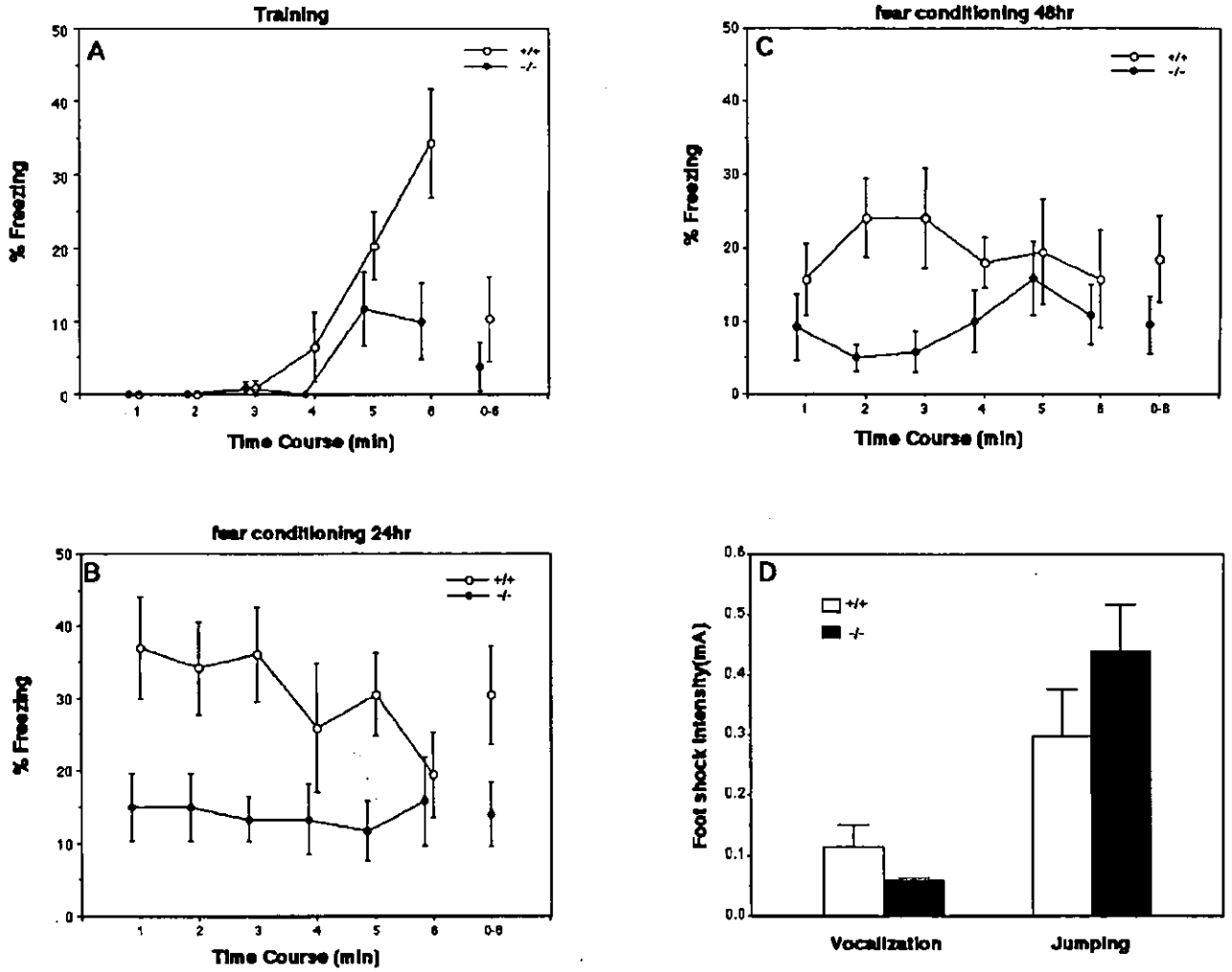

FIG. 6. Contextual fear conditioning task of the wild-type and homozygous BTEB$^{-/-}$ mutant mice. (A) Mean percentages of freezing before and during three foot shocks were determined at 5-s intervals. Three 1-s foot shocks (0.5 mA) were given 3, 4, and 5 min after animals had been placed in a new foot shock-equipped chamber. (B) Mean percentages of freezing behavior of the animals 24 h after the footshock. The foot shock-treated animals in panel A were returned to their original cages for 24 h. Immediately the animals were returned to the footshock chamber, the percentages of freezing behavior of the mice were counted. (C) After the experiments in panel B, the mice were returned to their original cage for another 24 h and then subjected to the same task as in panel B. Observations were carried out by using a time-sampling procedure. For every 5 s, each mouse was judged as either freezing or active during the test. The values were expressed as the average percentages of the mice used for each group with minimal deviations. (D) Sensitivity to foot shock. Sensitivity to foot shock was quantified by measuring minimal levels of current required to elicit two stereotypical behaviors: vocalization and jumping. In each experiment, wild-type mice (n = 9) and homozygous mice (n = 11) were used.

ebellar function (Fig. 5A). In addition to the general activities described, gait behavior (Fig. 5B), horizontal wire hanging (Fig. 5C), and rod walking (Fig. 5D) were examined as the basis of the rotorod test. In these tests, homozygous BTEB$^{-/-}$ mutant and wild-type mice did not show so much difference as to physically affect the rotorod test. In this task, animals must make continuous adjustments to their balance and posture in order to keep upright on a rod rotating at a constant velocity during each 5-min trial. In general, the BTEB$^{-/-}$ mice (n = 9) exhibited a significant performance deficit compared with the heterozygous BTEB$^{+/-}$ mutant mice (n = 14) (Fig. 5A). On the first day of the experiment, no mouse could stay on the rotating rod for a long time, regardless of the genotype. However, while days of training clearly improved the adjustment performance of heterozygous mice, BTEB$^{-/-}$ mice did not show improved performance in the rotorod test after daily training. These data suggest that the basis of the performance deficit of BTEB$^{-/-}$ mice on the rotorod test is in motor learning and motor coordination (Fig. 5A).

(iii) Contextual fear conditioning. BTEB is also distinctly expressed in the hippocampus and amygdala (Fig. 3). Since contextual fear conditioning requires correct functioning of both the hippocampus and amygdala, we tested BTEB$^{-/-}$ mice in context-dependent fear conditioning (Fig. 6). Fear conditioning is based on the ability of normal animals to fear a previous neural stimulus, or conditioned stimulus, because of

its temporal association with an adverse stimulus such as a foot shock. When reexposed to the conditioned stimulus, conditioned animals tend to refrain from all but respiratory movement, a response known as freezing. The percentage of time spent in freezing was quantified. During the conditioning phase of the experiment, mice were placed in the shock chamber and received three 1-s foot shocks at 1-min intervals. In the early phase of the experiment, before the first foot shock, a baseline activity was assessed for the $BTEB^{-/-}$ mutant and wild-type mice. Baseline fear during the first 3 min was characteristically low and did not differ across genotype (Fig. 6A). When foot shocks were given to the mice, both wild-type and $BTEB^{-/-}$ mutant groups showed significantly increased freezing behavior during training, although $BTEB^{-/-}$ mice appeared to be slightly more defective in their freezing response compared to the wild type (Fig. 6A). After the three foot shocks, the experimental animals were returned to their original cages. After 20 h, mice were placed in the same conditioning chamber and monitored for freezing behavior, which was characterized by an immobile and crouching posture. Both $BTEB^{-/-}$ mutant and wild-type mice displayed the conditioned freezing response in the training context. However, mutants froze significantly less than did the wild-type mice, indicating a moderate deficit in context-dependent fear conditioning (Fig. 6B). The mice under examination were again returned to their original cages. After an additional 24 h, the mice were again subjected to the test of contextual fear conditioning. Although mice with a wild-type BTEB genotype again displayed the conditioned freezing response, albeit to a lesser extent than the previous trial, the $BTEB^{-/-}$ mutant mice still showed a significant deficit in contextual freezing response relative to the wild-type mice (Fig. 6C). We then tested whether or not $BTEB^{-/-}$ mice have an altered nociceptive reaction to shock, because changes in pain sensitivity can affect performance on the fear conditioning test. For both $BTEB^{-/-}$ and wild-type mice, we determined the threshold current for eliciting two progressive reactions, jumping and vocalization, in response to increasing electrical foot shocks (Fig. 6D). The results of these experiments showed that there was little difference, if any, in the jumping and vocalization reaction between the $BTEB^{-/-}$ mutant and wild-type mice. The level of current required to induce vocal responses from the $BTEB^{-/-}$ mice (0.058 ± 0.006 mA) was a little lower than that for the wild-type mice [0.114 ± 0.036 mA; $F(1,17) = 1.72$, $P = 0.207$], whereas the reverse was observed in the jumping behavior [0.30 ± 0.08 mA for wild-type mice and 0.44 ± 0.08 mA for $BTEB^{-/-}$ mutants; $F(1,17) = 1.72$, $P = 0.207$]. These data indicated that the pain sensitivity and physical response to pain were not so different between the wild-type and $BTEB^{-/-}$ mutant mice and thus were not considered to affect performance in fear conditioning.

DISCUSSION

BTEB belongs to the Sp1/XKLF family of transcription factors with characteristic triple repeat C2H2 zinc finger motifs (15). Despite their similarity in primary structure and DNA-binding property, these factors have unique functions. It has been demonstrated from gene targeting experiments that Sp1-, Sp3-, and Sp4-deficient mice display very different phenotypes. Retarded development was observed in $Sp1^{-/-}$ mutant embryos, and they showed a broad range of abnormalities, resulting in embryonic death around day 11 of gestation. The expression of many putative target genes, including cell cycle-regulated genes, was not significantly affected in $Sp1^{-/-}$ embryos, except for reduced MeCP2 expression (22). On the other hand, Sp3 deficiency resulted in embryonic growth retardation and neonatal death because of respiratory failure, the cause of which remains obscure (2). Histological examinations of various organs of the $Sp3^{-/-}$ mutant mice revealed a pronounced defect in late tooth formation due to an impaired dentin or enamel layer of the developing teeth. In $Sp4^{-/-}$ mutant mice, postnatal death occurred in two of the neonates within the first few days. The remaining $Sp4^{-/-}$ mutants showed retarded growth compared to wild-type littermates, and males were defective in reproduction (31). Compared to Sp1, BTEB is a smaller protein consisting of 244 amino acids with a high sequence similarity to Sp1 in the zinc finger domain and has a closely similar binding affinity toward the GC-box sequence (15). As described previously, however, unique properties of translational regulation and T_3-inducible expression of BTEB prompted us to produce BTEB-defective mice to aid understanding of the physiological roles of BTEB and, at least, a part of the function of thyroid hormone T_3. Matings between heterozygous $BTEB^{+/-}$ mutant mice gave female and male $BTEB^{-/-}$ pups according to normal Mendelian genetics, and these animals grew apparently normally and were fertile. BTEB expression was first observed in the tip of the nasal bone at E12.5, and expression continued to spread throughout various tissues and organs up until parturition. Generally speaking, BTEB was expressed ubiquitously in adult animals and displayed characteristically potent expression in the hippocampus, cerebellum, and bone. By comparing β-Gal staining between $BTEB^{-/-}$ and $BTEB^{+/-}$ mice, we investigated whether BTEB deficiency caused any abnormality in organogenesis, paying special attention to the skeleton, hippocampus, and cerebellum. However, we could not find any gross morphological alterations in these tissues of $BTEB^{+/-}$ and $BTEB^{-/-}$ mice. Immunostaining with anti-IP_3R1 antibody showed that dendrites sprouting from Purkinje cells appeared to be slightly decreased in $BTEB^{-/-}$ mice. Although this seems to be consistent with the enhanced neurite outgrowth seen with overexpression of BTEB in Neuro-2A cells (4), precise quantitative analysis of the dendrite formation needs to be carried out by other methods such as electron microscopy. These results imply that BTEB is not involved in the gross morphogenesis of these organs at the light microscopic level or that other members of the Sp family may be compensating for the $BTEB^{-/-}$ deficiency.

On the other hand, we found that mouse behavior was significantly affected by BTEB deficiency. Detailed and systematic analyses in gross neurological and motor tasks of the $BTEB^{-/-}$ mutants revealed only slight differences in locomotor activities, rearing behavior, and speed of movement or no difference in the rod-walking test, light-dark choice test, horizontal wire-hanging test, or gait measurements compared to wild-type mice. However, we observed a performance deficit in $BTEB^{-/-}$ mice on the rotating rod, a test considered to involve the function of the cerebellum. Although sensorimotor learning and, therefore, performance on the rotarod cannot easily

be attributed to a single brain region, it is widely accepted that the cerebellum is a major component involved in this task (19). Mice with structural abnormalities in the cerebellum or with disruptions in genes richly expressed in the cerebellum exhibit performance deficits on the rotorod (17, 30). The performance deficit of BTEB$^{-/-}$ mice in the rotorod test is consistent with the defective function of BTEB that showed enhanced expression in the cerebellum. In the cerebellum, dynamic BTEB expression was initiated at P7, around the time when synapse formation starts to mature in the mouse brain (8). The formation of the synapses in BTEB$^{-/-}$ mice should be quantitatively analyzed in more detail to see whether the defective rotorod performance of BTEB$^{-/-}$ mice is due to impaired synapse formation.

In connection with the marked expression of BTEB in the pyramidal cell layers of the hippocampus, the BTEB$^{-/-}$ mice displayed a marked defect in contextual freezing response. The freezing deficit of the mutant mice was observed both immediately (immediate after shock freezing) and 1 day (delayed freezing) after the shock was presented. Since several control experiments indicated that BTEB deficiency caused neither a sensory nor a motor performance deficit in the response to foot shock, this result implies that BTEB$^{-/-}$ mice have deficits in the acquisition and preservation of memory. Although various brain areas are considered to be implicated in the process of contextual fear conditioning, the neural circuits of the hippocampus and amygdala, in particular, are responsible for contextual fear conditioning (1, 7, 16, 25). Since BTEB expression increased in the pyramidal cells of the hippocampus at P7 when synapses began to mature in the brain, it is possible that the impaired fear response in the BTEB-deficient mice resulted from impaired synapse formation in the hippocampus. The possible involvement of BTEB in synapse formation is supported by the enhanced neurite outgrowth of Neuro-2A cells resulting from the overexpression of BTEB (4). Additional experiments, such as the water maze test (23) and the conditioning taste aversion test (21, 36), are necessary to determine whether BTEB deficiency causes defective neural processes that are dependent on the hippocampus, the amygdala, or both. It would also be worthwhile and interesting to investigate the target genes of BTEB for further understanding the function of BTEB itself and, at least, a part of T_3 function in the development of the central nervous system. The distinct behavioral abnormalities of the BTEB knockout mice and characteristic expression pattern of BTEB will provide a useful system for further investigation of the mechanisms underlying motor function, learning, and memory.

ACKNOWLEDGMENTS

We thank T. Sakurai, T. Nakamura (Institute of Basic Medical Sciences, University of Tsukuba) and H. Ogura (Tsukuba Research Laboratories, Eisai Co., Ltd.) for valuable discussion and advice and S. Okamura (Graduate School of Biomedical Sciences, Hiroshima University) for technical assistance. The antibody against IP3R1 was kindly donated by K Mikoshiba (Department of Molecular Neurobiology, Institute of Medical Science, University of Tokyo). We thank T. O'Connor (TARA Center, University of Tsukuba) for critical reading of the manuscript and advice, D. Mori (Graduate School of Life Science, Tohoku University) and N. Suzuki (TARA Center, University of Tsukuba) for help in experiments, and S. Suzuki (Graduate School of Life Science, Tohoku University) and Y. Nemoto (TARA Center, University of Tsukuba) for clerical assistance.

This work was supported in part by Grants-in-Aid for Scientific Research (B) from the Ministry of Education, Science, Sports, and Culture of Japan and by grants from Core Research for Evolutionary Science and Technology, Japan Science and Technology, and Sankyo Co., Ltd.

REFERENCES

1. **Anagnostares, S. G., S. Maron, and M. S. Fenselow.** 1999. Temporally graded retrograde amnesia of contextual fear after hippocampal damages in rats: within-subject exmination. J. Neurosci. 19:1106–1114.
2. **Bouwman, P., H. Gollner, H. P. Elsasser, G. Eckhoff, A. Karis, F. Grosveld, S. Philipsen, and G. Suske.** 2000. Transcription factor Sp3 is essential for post-natal survival and late tooth development. EMBO J. 19:655–661.
3. **Brown, D. D., Z. Wang, J. D. Furlow, A. Kanamori, R. A. Schwartzman, B. F. Remo, and A. Pinder.** 1996. The thyroid hormone-induced tail resorption program during *Xenopus laevis* metamorphosis. Proc. Natl. Acad. Sci. USA 93:1924–1929.
4. **Denver, R. J., L. Ouellet, D. Furling, A. Kobayashi, Y. Fujii-Kuriyama, and J. Puymirat.** 1999. Basic transcription element-binding protein (BTEB) is a thyroid hormone-regulated gene in the developing central nervous system: evidence for a role in neurite outgrowth. J. Biol. Chem. 274:23128–23134.
5. **Denver, R. J., S. Pavgi, and Y. B. Shi.** 1997. Thyroid hormone-dependent gene expression program for *Xenopus* neural development. J. Biol. Chem. 272:8179–8188.
6. **Ferguson, G. D., S. G. Anagnostaras, A. J. Silva, and H. R. Herschman.** 2000. Deficit in memory and motor performance in synaptotagmin IV mutant mice. Proc. Natl. Acad. Sci. USA 97:5598–5603.
7. **Frankland, P. W., V. Cestari, R. K. Filipkowski, R. J. McDonald, and A. J. Silva.** 1998. The dorsal hippocampus is essential for context discrimination but not for contextual conditioning. Behav. Neurosci. 112:863–874.
8. **Gaarskjaer, F. B.** 1985. The development of the dentate area and the hippocampal mossy fiber projection of the rat. J. Comp. Neurol. 24:1154–1170.
9. **Hogan, B., R. Beddington, F. Constantini, and E. Lacy.** 1994. Manipulating the mouse embryo: a laboratory manual, p. 277–290. Cold Spring Harbor Laboratory, Cold Spring Harbor, N.Y.
10. **Iglesias, T., A. Caubin, G. H. Stunnenberg, A. Zaballos, J. Bernal, and A. Minoz.** 1996. Thyroid hormone-dependent transcriptional repression of neural adhesion molecule during brain maturation. EMBO J. 15:4307–4316.
11. **Iglesias, T., A. Caubin, J. Zaballos, J. Berna, and A. Munoz.** 1995. Identification of mitochondrial NADH dehydrogenes submit 3(ND3) as a thyroid hormone regulated gene by whole genome PCR analysis. Biochem. Biophys. Res. Commun. 210:995–1100.
12. **Ikegami, S.** 1994. Behavioral impairment in radial-arm maze learning and acetylcholine content of the hippocampus and cerebral cortex in aged mice. Behav. Brain Res. 65:103–111.
13. **Ikegami, S., A. Harada, and N. Hirokawa.** 2000. Muscle weakness, hyperactivity, and impairment in fear conditioning in tau-deficient mice. Neurosci. Lett. 279:129–132.
14. **Imataka, H., K. Nakayama, K. Yasumoto, A. Mizuno, Y. Fujii-Kuriyama, and M. Hayami.** 1994. Cell-specific translational control of transcription factor BTEB expression. The role of an upstream AUG in the 5′-untranslated region. J. Biol. Chem. 269:20668–20673.
15. **Imataka, H., K. Sogawa, K. Yasumoto, Y. Kikuchi, K. Sasano, A. Kobayashi, M. Hayami, and Y. Fujii-Kuriyama.** 1992. Two regulatory proteins that bind to the basic transcription element (BTE), a GC box sequence in the promoter region of the rat P-4501A1 gene. EMBO J. 36:63–71.
16. **Kim, J. J., and M. S. Fanselow.** 1992. Modality-specific retrograde amnesia of fear. Science 256:675–677.
17. **Lalonde, R., A. N. Bensoula, and M. Filali.** 1995. Rotorod sensorimotor learning in cerebellar mutant mice. Neurosci. Res. 42:3–6.
18. **Legrand, J.** 1983. Thyroid hormones and maturation of the nervous system. J. Physiol. 78:603–652.
19. **Llinas, R., and J. P. Welsh.** 1993. On the cerebellum and motor learning. Curr. Opin. Neurobiol. 9:58–65.
20. **Mangelsdorf, D. J., C. Thummel, M. Beato, P. Herrlich, G. Schutz, K. Umesono, B. Blumberg, P. Kastner, M. Mark, P. Chambon, and R. M. Evans.** 1995. The nuclear receptor superfamily: the second decade. Cell 83:835–839.
21. **Masugi, M., M. Yokoi, R. Shigemoto, K. Muguruma, Y. Watanabe, G. Sansig, H. Van der Putten, and S. Nakanishi.** 1999. Metabstrozic glutamate receptor subtype 7 ablation causes deficit in fear response and conditioned taste axpression. J. Neurosci. 19:55–63.
22. **Marin, M., A. Karis, P. Visser, F. Grosveld, and S. Philipsen.** 1997. Transcription factor Sp1 is essential for early embryonic development but dispensable for cell growth and differentiation. Cell 89:619–628.
23. **Morris, R. G., P. Garrud, J. N. Rawlins, and J. O'Keefe.** 1982. Place navigation impaired in rats with huppocampol lesions. Nature 297:681–683.
24. **Munoz, A. A., A. Rodriguez-Pena, A. Perez-Castillo, B. Ferreiro, J. G. Sutcliffe, and J. Bernal.** 1991. Effect of neonatal hypothyroidism on rat brain gene expression. Mol. Endocrinol. 5:273–280.
25. **Phillips, R. G., and J. E. LeDoux.** 1985. Differential contribution of amygdala

and hippocampus to cued and contextual fear conditioning. Behav. Neurosci. 106:274–285.
26. **Porterfield, S. P., and C. E. Hendrich.** 1993. The role of thyroid hormones in prenatal and neonatal neurological development: current perspectives. Endocrinol. Rev. 14:94–106.
27. **Ryo, Y., A. Miyawaki, T. Furuichi, and K. Mikoshiba.** 1993. Expression of the metabolic glutamate receptor mGluR1 alpha and the ionotropic glutamate receptor GluR1 in the brain during postnatal development of normal mouse and in the cerebellum from mutant mice. J. Neurosci. Res. 36:19–32.
28. **Sambrook, J., E. F. Fritsch, and T. Maniatis.** 1989. Molecular cloning: a laboratory manual, 2nd ed. Cold Spring Harbor Laboratory Press, Cold Harbor, N.Y.
29. **Sogawa, K., Y. Kikuchi, H. Imataka, and Y. Fujii-Kuriyama.** 1993. Comparison of DNA-binding properties between BTEB and Sp1. J. Biochem. 114: 605–609.
30. **Storm, D. R., C. Hansel, B. Hacker, A. Parent, and D. J. Linden.** 1998. Impaired cerebellar long-term potentiation in type I adenylyl cyclase mutant mice. Neuron 1:199–210.
31. **Supp, D. M., D. P. Witte, W. W. Branford, E. P. Smith, and S. S. Potter.** 1996. Sp4, a member of the Sp1-family of zinc finger transcription factors, is required for normal murine growth, viability, and male fertility. Dev. Biol. 176:284–299.
32. **Thompson, C. C.** 1996. Thyroid hormone-responsive genes in developing cerebellum include a novel synotogamine and a hairless homolog. J. Neurosci. 16:7832–7840.
33. **Tsai, M. J., and B. W. O'Malley.** 1994. Molecular mechanisms of action of steroid/thyroid receptor superfamily members. Annu. Rev. Biochem. 63: 451–486.
34. **Ussault, J. H., and J. Ruel.** 1987. Thyroid hormones and brain development. Annu. Rev. Physiol. 49:321–334.
35. **Vega-Nunez, E., R. Menendez-Hurtado, A. Garesse, A. Santos, and A. Perez-Castillo.** 1995. Thyroid hormone-regulate brain mitochondrial genes revealed by differential cDNA cloning. J. Clin. Investig. 89:3–9.
36. **Yamamoto, T., Y. Fujimoto, T. Shimura, and N. Sakai.** 1995. Conditioned taste aversion in rats with excitotoxic brain lesion. Neurosci. Res. 22:31–49.

TOXICOLOGICAL SCIENCES 72, 84–91 (2003)
DOI: 10.1093/toxsci/kfg002

TCDD Treatment Eliminates the Long-Term Reconstitution Activity of Hematopoietic Stem Cells

Ruriko Sakai,*†‡ Teruyuki Kajiume,*†‡ Hiroko Inoue,*‡ Rieko Kanno,*‡ Masaki Miyazaki,*‡ Yuichi Ninomiya,*‡ and Masamoto Kanno*‡[1]

*Department of Immunology, Graduate School of Biomedical Science, Hiroshima University, Minami-ku, Hiroshima 734-8551, Japan; †Japanese Society for the Promotion of Science Research Fellowship for Young Scientists; and ‡CREST (Core Research for Evolutional Science and Technology) of Japan Science and Technology Corporation, Kawaguchi, Saitama 332-0012, Japan

Received September 30, 2002; accepted November 11, 2002

2,3,7,8-Tetrachlorodibenzo-*p*-dioxin (TCDD), an endocrine disrupting chemical (EDC), can cause carcinogenesis, immunosuppression, and teratogenesis, through a ligand-activated transcription factor, the aryl hydrocarbon receptor (AhR). Despite remarkable recent advances in stem cell biology, the influence of TCDD on hematopoietic stem cells (HSCs), which possess the ability to reconstitute long-term multilineage hematopoiesis, has not been well investigated. In this study we examined the influence of TCDD on HSCs enriched for $CD34^-$, c-kit^+, Sca-1^+, lineage negative ($CD34^-$KSL) cells. The number of the $CD34^-$KSL cells was found to be increased about four-fold upon a single oral administration of TCDD (40 μg/kg body weight). Surprisingly, we found that these TCDD-treated cells almost lost long-term reconstitution activity. This defect was not present in *AhR*$^{-/-}$ mice. These findings suggest that modulation of AhR/ARNT system activity may have an effect on HSC function or survival.

Key Words: **2,3,7,8-tetrachlorodibenzo-*p*-dioxin; TCDD; hematopoietic stem cells (HSCs); $CD34^-$KSL ($CD34^-$, c-kit^+, Sca-1^+, lineage negative) cells; long-term reconstitution activity; aryl hydrocarbon receptor; AhR.**

In recent years, many reports have focused on certain man-made toxins known as endocrine disrupting chemicals (EDCs) that persist in the environment and are capable of altering the endocrine homeostasis of animals, causing serious reproductive and developmental defects (Birnbaum, 1995; Sweeney, 2002). One such compound is the xenobiotic agent 2,3,7,8-tetrachlorodibenzo-*p*-dioxin (TCDD), one of the most potent members of a family of EDCs, the polyhalogenated aromatic hydrocarbons. TCDD exposure can result in carcinogenesis, immunosuppression, and tissue and organ toxicity, as well as teratogenesis (Couture *et al.*, 1990; Peters *et al.*, 1999).

TCDD is believed to exert its effects primarily through a ligand-activated transcription factor, the aryl hydrocarbon receptor (AhR). AhR belongs to the basic helix–loop–helix (bHLH) superfamily of DNA binding proteins and heterodimerizes with the AhR nuclear translocator (ARNT) to form an AhR/ARNT transcription factor complex (Hoffman *et al.*, 1991; Reyes *et al.*, 1992). This complex binds to specific DNA sites in the regulatory domains of numerous target genes and mediates the biological effects of exogenous ligands (Okey *et al.*, 1994). Indirubin and indigo were reported recently as potent natural ligands of AhR (Adachi *et al.*, 2001). Studies using TCDD and its related congeners that activate AhR also suggest that the receptor has immunological functions. The recent generation of *AhR* knockout mice has provided evidence of a role for this protein in hepatic fibrosis development and in the immune system (Fernandez-Salguero *et al.*, 1995; Mimura *et al.*, 1997; Schmidt *et al.*, 1996). Although it is also known that AhR is present in most cell and tissue types of the body, its functions in hematopoietic stem cells (HSCs) have not been examined in detail.

HSCs possess the ability to self-renew or differentiate into multiple distinct cell lineages. Substantial HSC self-renewal has been demonstrated in transplantation models (Iscove and Nawa, 1997; Pawliuk *et al.*, 1996), in stroma-containing long-term marrow cultures supplemented with thrombopoietin (Yagi *et al.*, 1999) and upon the ectopic expression of *HOXB4* (Antonchuk *et al.*, 2002; Sauvageau *et al.*, 1995). Although there are some reports that *in vitro* HSC self-renewal has been achieved using various culture conditions (Audet *et al.*, 2001; Ema *et al.*, 2000; Holyoake *et al.*, 1996; Miller and Eaves, 1997), the processes that govern HSC self-renewal remain poorly understood. Although the functional diversity of HSCs has been demonstrated unequivocally, it is less clear how such diversity is generated. The prevailing view is that HSC heterogeneity is regulated by both extrinsic and intrinsic events (Enver *et al.*, 1998; Metcalf, 1998). Extrinsic (environmental) signals are derived predominantly from stromal cells and their products. Stromal cells are organized into niches that differ in their ability to maintain HSCs (Blazsek *et al.*, 1995; Wineman *et al.*, 1996). Thus, homing of HSCs to different types of

[1] To whom correspondence should be sent at Department of Immunology, Graduate School of Biomedical Science, Hiroshima University, 1-2-3, Kasumi, Minami-ku, Hiroshima 734-8551, Japan. Fax: +81-82-257-5179. E-mail: mkanno@hiroshima-u.ac.jp.

stromal cell niches should contribute to HSC heterogeneity. In addition to extrinsic signals, intrinsic mechanisms control HSC decisions. Intrinsic mechanisms could induce HSC heterogeneity if HSCs make random decisions at the time of each HSC division. For example, each HSC has a choice of many fates, including self-renewal, differentiation, apoptosis, and migration. Evidence for stochastic processes comes from the analysis of the differentiation of myeloid and lymphoid precursors (Busslinger *et al.*, 2000; Ogawa, 1999). For example, multipotent myeloid precursors generate more restricted precursors in an apparently random fashion (Ogawa, 1999). Recent studies of murine HSCs clearly demonstrated that expression of the surface antigens of stem cells is under the influence of the developmental stage and the kinetic state of the stem cells (Ogawa, 2002). It was demonstrated using the monocloncal anti-CD34 antibody RAM34 that only the $CD34^-$ fraction of lineage negative (Lin^-), Sca-1^+, c-kit^+ bone marrow (BM) cells, known as $CD34^-$KSL cells, of normal adult mice are capable of long-term hematopoietic reconstitution in lethally irradiated mice (Osawa *et al.*, 1996).

Surprisingly, there have been only a few reports concerning the relationship between HSC and TCDD that describe an increase in the number of hematopoietic progenitor cells upon TCDD treatment (Frazier *et al.*, 1994; Murante and Gasiewicz, 2000; Staples *et al.*, 1998; Thurmond and Gasiewicz, 2000). Therefore, we decided to investigate more precisely whether TCDD influences the long-term reconstruction activity of $CD34^-$KSL cells in BM.

MATERIALS AND METHODS

Chemicals. 2,3,7,8-Tetrachlorodibenzo-*p*-dioxin (> 99% pure) was obtained from Cambridge Isotope Laboratories Inc. (Cambridge, MA). The compound was dissolved in corn oil as an administration vehicle (Katayama Chemicals, Inc., Chuo, Osaka, Japan).

Animals. C57BL/6J (B6, CD45.2) mice were obtained from CREA JAPAN, INC. (Meguro, Tokyo, Japan) and B6 SJL *Ptprc*^{a} *Pep3*^{b}BoyJ (B6 *Ptprc*, CD45.1) mice were obtained from Jackson Laboratory (Bar Harbor, ME) and kept in accordance with the Laboratory Animal Science guidelines of Hiroshima University. *AhR*$^{-/-}$ mice were kindly provided by Dr. Y. Fujii-Kuriyama (Tohoku University, Sendai, Japan). All mice were acclimated in-house for one week prior to treatment. Mice older than 10 weeks of age were used in the experiments.

TCDD treatment. The experiments shown here were performed more than three times with at least five mice per group. Animals were administered either vehicle or TCDD at day zero and were euthanized at h 0, 3, and 12, and on days 1, 3, 7, 14, 28, 56, and 112. TCDD-treated animals were administered by gavage 40 μg/kg body weight (bw) TCDD and vehicle-treated animals were administered by gavage an equivalent dose of corn oil. The following TCDD doses were used: 0 (vehicle), 0.16, 0.63, 2.5, 10, 40, and 80 μg/kg bw. Animals were administered either vehicle or TCDD at day zero and were euthanized on day 7.

Antibodies. The antibodies used in immunofluorescence staining included RAM34 (anti-CD34), D7 (anti-Sca-1), 2B8 (anti-c-kit), 104 (anti-CD45.2), and A20 (anti-CD45.1). Antibodies using for lineage markers included RA3-6B2 (anti-CD45R/B220), 145-2C (anti-CD3e), RM4-5 (anti-CD4), 53-6.7 (anti-CD8a), M1/70 (anti-Mac-1), RB6-8C5 (anti-Gr-1), and TER119. All the antibodies were purchased from Pharmingen (San Diego, CA).

Purification and analysis of $CD34^-$KSL cells. BM cells were flushed from femurs and tibiae of mice. Cell suspensions were then filtered through a sterile 100 μm Cell Strainer (No. 2360; Falcon, Lincoln Park, NJ) and stained with biotinylated antilineage makers. For analysis, cells were then stained with fluorescein isothiocyanate (FITC) anti-CD34, phycoerythrin (PE) anti-Sca-1, allophycocyanin (APC) anti-c-kit antibodies and streptavidin-PerCP (Pharmingen). Four-color analysis was performed on a FACS Calibur (Becton Dickinson, San Jose, CA) using CELLQuest software (Becton Dickinson). For cell sorting, bone marrow was depleted of lineage positive cells using MACS (Milteny Biotech GmbH, Bergisch Gladbach). Cells were stained with biotinylated antilineage markers and then were allowed to bind streptavidin-magnetic beads (Milteny Biotech). Ten μl of beads were used per 10^7 cells. Cells were then applied to a C-type MACS column and nonadherent (lineage negative; Lin^-) cells were stained with the subsequent antibodies as described above (Randall and Weissman, 1998). $CD34^-$KSL cells were sorted by FACS Vantage SE (Becton Dickinson). Dead cells were excluded by propodium iodide (PI) from analysis and sorting.

Competitive repopulation assay. We applied and performed a competitive repopulation assay to which the CD45 (Ly5) system was adapted (Ema and Nakauchi, 2000); 100 sorted $CD34^-$KSL cells from TCDD- or vehicle-treated B6 (CD45.2), *AhR*$^{-/-}$ (CD45.2), and *AhR* WT (CD45.2) mice were mixed with 1×10^5 BM competitor cells (B6 *Ptprc*, CD45.1) and were transplanted into B6 *Ptprc* mice irradiated at a dose of 10 Gy. After transplantation, peripheral blood cells of the recipients were stained with FITC anti-CD45.2 and PE anti-CD45.1. The cells were simultaneously stained with biotinylated anti-B220 or biotinylated anti-TER119, a mixture of biotinylated anti-Mac-1 and Gr-1, or a mixture of APC-conjugated anti-CD4 and -CD8. Biotinylated antibodies were developed with streptavidin-APC (Molecular Probes, Eugene, OR). The cells were analyzed on a FACS, and percentage chimerism was taken as the quadrant ratio of donor cells ($CD45.2^+$ cells). When percent chimerism was more than 1% with all lineage reconstitution, recipient mice were considered to be multilineage reconstituted (positive mice). Dead cells were excluded by PI staining.

Two step single cell-methylcellulose colony assay. Sorted $CD34^-$KSL cells were deposited as single cells into 96-well microtiter plates by FACS Vantage SE and Clone Cyt (Becton Dickinson). The single cells were incubated in 100 μl of culture medium (Methocult™ GF, StemCell Technologies Inc., Vancouver, British Columbia, Canada) at 37°C in a humidified atmosphere 5% CO_2 for seven days. Cultures were scored for colony-forming units using an inverted microscope. We evaluated and designated those containing more than 50 cells/colony as first colonies. Next, the first colonies were collected and sorted to deposit 100 cells/well and incubated for another seven days. Cultures were scored for colony-forming units in the same manner, and these colonies were designated second colonies.

Statistical analysis. Means ± SD were compared with a Student's *t*-test. Significance levels were set at $p = 0.01$–0.05 (*), $p = 0.01$–0.001 (**), and $p < 0.001$ (***).

RESULTS

The Number of $CD34^-$KSL Cells Was Increased by TCDD

To understand the effects of TCDD on the immune and/or hematopoietic systems, we focused on the study of HSCs in adult BM. Although recent studies reported that the number of hematopoietic progenitor cells was increased by TCDD administration (Murante and Gasiewicz, 2000), our first question was whether multilineage long-term HSCs are really affected by TCDD. Therefore, we investigated more precisely the effects of TCDD on long-term HSC populations, $CD34^-$KSL cells, in BM. We treated 10-week-old C57BL/6 mice with 40 μg/kg bw

TCDD or corn oil (vehicle) by single oral administration, and assessed HSC characteristics after seven days. When the lineage negative BM cells were further developed with Sca-1/c-kit, the percentage of Sca-1$^+$/c-kit$^+$ cells (gated in Fig. 1A) from TCDD-treated mice was found to be higher (7.73%) than that of cells isolated from vehicle-treated mice (2.32%). This observation is in good agreement with a recent report (Murante and Gasiewicz, 2000). We then assessed the percentages and cell number of the long-term HSC population as indicated by the CD34 marker. The percentage of CD34-negative cells was higher in TCDD-treated (12.21%) compared to vehicle-treated (4.44%) mice (Fig. 1A). Although there were no significant differences in the total number of BM cells between vehicle- and TCDD-treated mice, the number of CD34$^-$KSL cells was four-fold higher in TCDD-treated mice (Fig. 1B, $p = 0.0001$, $n = 20$). It has been reported that TCDD administration increases the number of KSL progenitor cells in dose-dependent fashion (Murante and Gasiewicz, 2000). In corroboration with these prior results, we also assessed and found that the increase in CD34$^-$KSL cells was TCDD dose-dependent at seven days after administration (Fig. 1C). The number of CD34$^-$KSL cells is increased with doses as low as 2.5 μg/kg bw and we fixed the experimental dose at 40 μg/kg bw on which the significant difference was seen (Fig. 1C, $p = 0.0083$, $n = 6$).

We next performed a time course analysis of the effects of a single oral administration of TCDD on CD34$^-$KSL hematopoietic stem cell populations. As shown in Figure 2, TCDD exposure increased the number of CD34$^-$KSL cells (Fig. 2B) from 12 h up to 56 days after treatment, although the number of total BM cells was not changed. Effects were observed as early as 12 h after treatment ($p = 0.0058$, $n = 5$), and peaked after about 1–2 weeks. Only after 112 days was this augmentation effect resolved. The increase in CD34$^-$KSL cells could be due to changes in a number of processes, cell proliferation, cell death, differentiation, and homing. We could not, however, find any significant differences in cell proliferation or cell death by BrdU and TUNEL assays, respectively (data not shown).

TCDD Treatment Abolishes the Stem Cell Function of the CD34$^-$KSL Cells

Next, we determined whether the TCDD-induced increased number of CD34$^-$KSL cells maintain normal stem cell function. We performed a competitive repopulation assay with CD45.2 mice as donors and CD45.1 mice as recipients (Fig. 3A and Materials and Methods). The peripheral blood (PB) cells of the recipient mice were assessed for the long-term reconstitution ability of donor cells every four weeks after 100 CD34$^-$KSL cells were transplanted. We monitored the reconstitution activity up to 28 weeks. In these experiments, "TCDD group" and "vehicle group" refer to recipient mice into which were transplanted CD34$^-$KSL cells from TCDD- and vehicle-treated mice, respectively.

First, the cellularity of recipient peripheral blood was measured and percentage chimerism (ratio of the donor CD45.2$^+$ cells) of nucleated PB cells was assayed with anti-CD45.2 and anti-CD45.1 monoclonal antibodies, as well as several lineage antibodies. Surprisingly, although the chimerism of the vehicle group was 20 to 80% (average 40%) after four months, we could not detect donor CD45.2$^+$ cells in the TCDD group with the exception of two mice (Figs. 3B and 3C). These results strongly suggest that the CD34$^-$KSL cells in TCDD-treated animals lose their hematopoietic long-term reconstitution activity.

To understand the mechanisms of this functional deterioration, we thought it could be a possibility that long-term reconstitution activity of HSC might shift from CD34$^-$KSL fraction to CD34$^+$KSL fraction, usually supporting short-term reconstitution activity, by stimulation of TCDD. One thousand CD34$^+$KSL cells from both TCDD- and vehicle-treated adult mice were transplanted by the same method as described above. No long-term reconstitution activity was observed in either group (data not shown). Therefore, it is reasonable to conclude that the effect of TCDD on long-term reconstitution activity is targeted on the CD34$^-$KSL cell itself rather than population shift.

Next we performed an *in vitro* two-step single-cell methylcellulose colony assay on CD34$^-$KSL cells to analyze the effects of TCDD on self-renewal activity at the single cell level. Single CD34$^-$KSL cells were sorted into individual wells filled with culture medium formulated to optimize the detection of murine hematopoieic progenitor cells, BFU-E, CFU-GM, CFU-G, CFU-M, and CFU-GEMM. Although we could not find a difference of cellularity of the colony between vehicle plates and TCDD plates (the plates where single CD34$^-$KSL cells from vehicle- or TCDD-treated mice were sorted into each well), the first colony forming ability of CD34$^-$KSL cells from the TCDD-treated mice was only one-third that of cells from the vehicle-treated mice (Fig. 3D, $p = 0.0024$, $n = 6$). Next we examined second colony forming activity. This process is an indicator of the self-renewal or progenitor-forming ability of HSCs. The second colony forming ability of CD34$^-$KSL cells from the TCDD-treated mice was one-tenth of that of vehicle-treated mice, and the size of colonies generated from CD34$^-$KSL cells from the TCDD-treated mice was 50% of that of vehicle-treated mice.

From these results, it is also conceivable that the long-term reconstitution activity of HSCs in CD34$^-$KSL populations is damaged by TCDD, despite the increase in cell number.

Absence of Aryl Hydrocarbon Receptor Prevents the Elimination of Stem Cell Activity

As AhR is known to be a major dioxin receptor, we also examined the role of AhR in the TCDD-mediated elimination of stem cell activity. We performed the same experiments as described above using *AhR*-knockout (*AhR*$^{-/-}$) mice. As shown

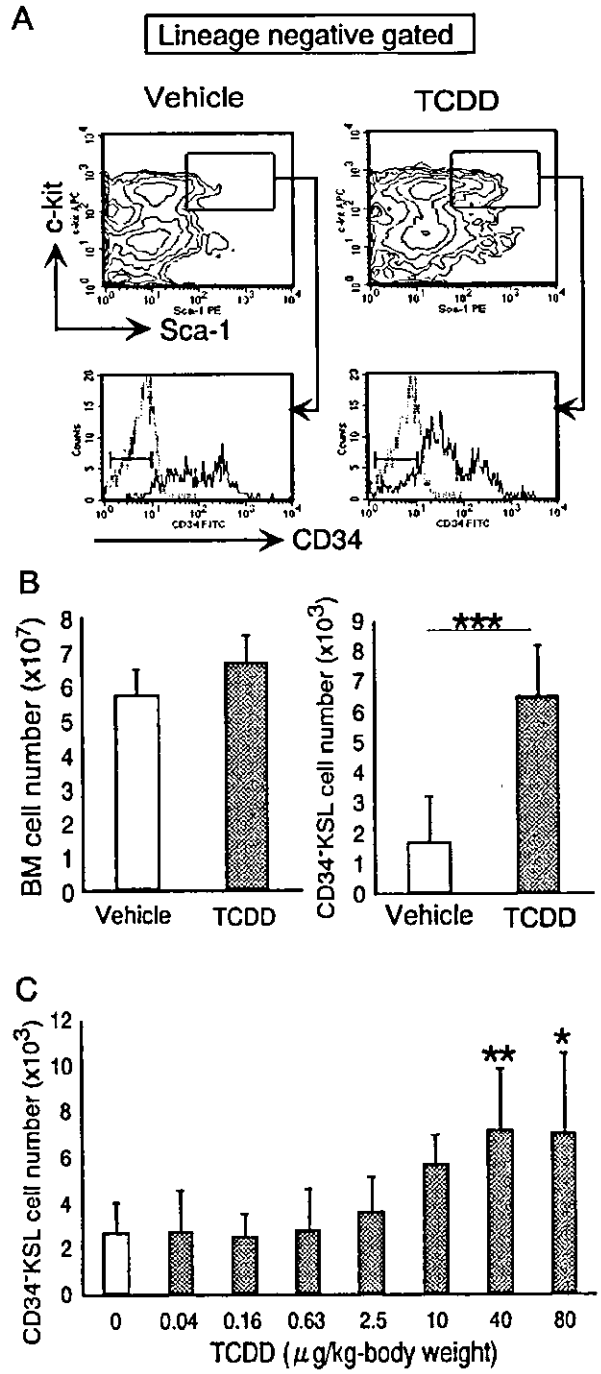

FIG. 1. Effects of TCDD on the number of BM cells and CD34$^-$KSL cells at day 7 following treatment, and dose-response profile of CD34$^-$KSL cells. (A) Flow cytometric analysis of CD34 expression profile on the KSL fraction of BM cells treated with vehicle (left panels) or TCDD (right panels). Representative flow cytometric counter plots of Sca-1/c-kit staining of lineage negative BM fractions (upper). Gated c-kit$^+$Sca-1$^+$Lin$^-$ (KSL) cells were examined for the expression of CD34. Fluorescence histogram (lower) shows CD34 staining profile of the gated, stem cell-enriched fraction. (B) The number of BM cells and CD34$^-$KSL cells from C57BL/6 (B6) mice treated with vehicle (open bar) or TCDD (filled bar) after seven days. Although there was no difference in the number of BM cells, a significant difference (***$p < 0.001$, $n = 20$) was seen in the number of CD34$^-$KSL cells. (C) Dose-response profile of the number of CD34$^-$KSL cells. 0 μg/kg bw indicates vehicle-treated control; **$p = 0.0083$ ($n = 6$) and *$p = 0.0482$ ($n = 5$) for 40 and 80 μg/kg bw, respectively. These experiments were performed more than 3 times with at least 5 mice per group.

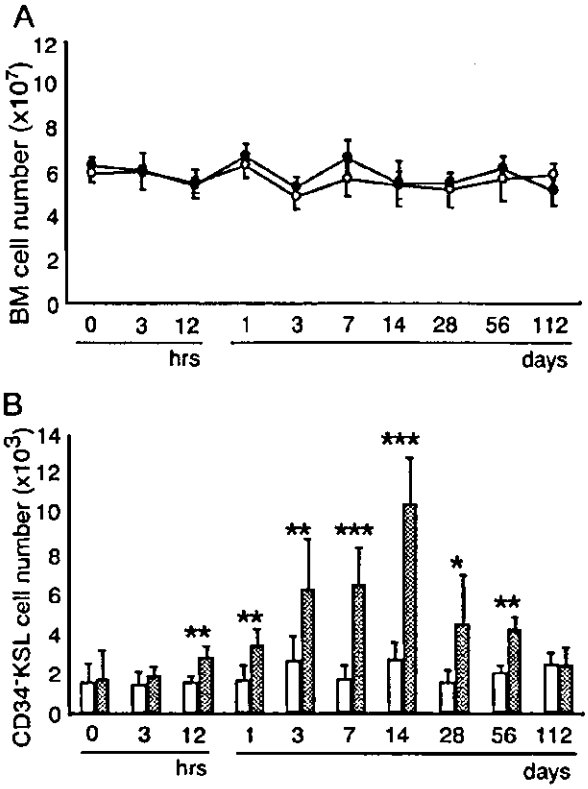

FIG. 2. Time course of BM and CD34$^-$KSL cells. The numbers of BM (A) and CD34$^-$KSL (B) cells were investigated at 0, 3, and 12 h, and at 1, 3, 7, 14, 28, 56, and 112 days following TCDD or vehicle treatment. No difference was seen in BM cell number at any timepoint between the vehicle- (open circles) or TCDD-treated (filled circles) groups. Significant differences were observed in CD34$^-$KSL cell number between the vehicle- (open bars) and TCDD-treated (filled bars) groups from 12 h on. At 14 days after treatment, the number of CD34$^-$KSL cells in the TCDD group was 3-fold that of the vehicle group. *p = 0.01 ~ 0.05; ** p = 0.001 ~ 0.001; *** $p < 0.001$. These experiments were performed more than 3 times with at least 5 mice per group.

in Figure 4A, we could not detect a significant TCDD-induced increase in the number of CD34$^-$KSL cells in $AhR^{-/-}$ mice, although a three- to four-fold increase in cell number was observed in wild type (WT) mice. It is noteworthy that the total number of BM cells was not changed between $AhR^{-/-}$ and WT mice.

Next, we performed the competitive repopulation assay to